Anuário do Instituto de Geociências
Universidade Federal do Rio de Janeiro
https://revistas.ufrj.br/index.php/aigeo/

ISSN 0101-9759
e-ISSN 1982-3908

Characterization and Geological Meaning of the Crystalline Basement Occurrence in the Unaí Region, Minas Gerais State (Central Brasilia Belt)

Caracterização e Significado Geológico da Ocorrência do Embasamento Cristalino na Região de Unaí, Minas Gerais (Faixa Brasília Central)

Florença das Graças Moura[1] & José Eloi Guimarães Campos[2]

[1]Instituto Federal de Goiás, Campus Goiânia, Goiânia, GO, Brasil
[2] Universidade de Brasília, Instituto de Geociências, Campus Universitário Darcy Ribeiro, Brasília, DF, Brasil
E-mails: fmouraunb@gmail.com; eloi@unb.br

Corresponding author: Florença das Graças Moura; fmouraunb@gmail.com

Abstract

Granitoid rocks petrographically and compositionally characterized as tonalite, monzonite granodiorite and granite were observed in restricted areas in the central portion of the external zone of the Brasilia Belt. These outcrops of peraluminous rocks were interpreted as the sialic basement of the region, associated with paleogeographic highs prior to the deposition of the Proterozoic sedimentary cover. U-Pb zircon age of 2.14 Ga and geochemical analysis are compatible with other Paleoproterozoic bedrock areas observed mainly in the north Brasilia Belt. The existence of a basement bulkhead conditioned the Neoproterozoic deformation, causing the inflection of regional structures from NNW to N60-70W and over again to the NNW regional trend. The absence of contact metamorphism along the adjacent supracrustal rocks, regional foliation attitude that is different from that observed in the granitoids (tonalite, granotiorite, monzonite and granite) and the older age, show that these rocks represent basement windows and not younger intrusive bodies, as previously interpreted. The rocks studied in this research are correlated to the Aurumina Suite, which represents the main basement rock set in the North Brasília Belt.

Keywords: Crystalline basement; Tonalite; Brasília Belt

Resumo

Granitoides caracterizados petrográfica e composicionalmente como tonalito, monzonito, granodiorito e granito foram observados em áreas restritas na porção central da zona externa da Faixa Brasília. Esses afloramentos foram interpretados como o embasamento siálico da região, caracterizados como altos paleogeográficos, anteriores à deposição da cobertura sedimentar proterozoica. A idade 2,14 Ga obtida pelo método U-Pb em cristais de zircão e as análises geoquímicas são compatíveis com rochas de embasamento que afloram principalmente na Faixa Brasília Norte. A existência de um alto do embasamento na porção externa da faixa condicionou a deformação Neoproterozoica, que causou a inflexão das estruturas regionais de NNW para N60-70W e novamente para a tendência regional NNW. A ausência de metamorfismo de contato ao longo das rochas supracrustais adjacentes, a foliação regional com atitude distinta daquelas observadas nos granitoides, e a idade de 2,14 Ga corrobora a hipótese de que as rochas de natureza tonalítica, monzonítica, granodiorítica e granítica são janelas de embasamento e não corpos intrusivos mais jovens, como anteriormente interpretados. As rochas estudadas neste trabalho são correlacionadas à Suíte Aurumina, que representa o principal conjunto de rochas do embasamento norte da Faixa Brasília.

Palavras-chave: Embasamento cristalino; Tonalito; Faixa Brasília

Received: 22 September 2021; Accepted: 26 July 2022

1 Introduction

The Tocantins Province (Almeida et al. 1981) is a Neoproterozoic orogenic system formed by the amalgamation of the Amazon, São Francisco and Paranapanema cratons during the Brasiliano Orogeny. This province is constituted of the Araguaia and Paraguay Belts bordering the Amazon Craton east and south, respectively, and the Brasília Belt that has developed on the western margin of the São Francisco Craton (Dardenne 2000).

Granitoid occurrences cropping out in restricted areas among the pelitic sediments at the base of the Bambuí Group were observed in the northwestern region of the Unaí town, in the State of Minas Gerais, Brazil. Initially, Rodrigues (2008) described a single outcrop that was interpreted as an intrusive tonalitic body dated as 785 ± 10 Ma and known as the "Arrependido Body".

Along the central-external zone of the Brasilia Belt there is no occurrence of basement rocks. The regional geologic maps demonstrate low grade metasedimentary rocks outcrop correlated to the Canastra, Paranoá, Vazante and Bambuí groups.

The aim of this paper is to describe and interpret the crystalline basement that crops out northwestern of Unaí town in the state Minas Gerais/Brazil (central Brasilia Belt), using geological, petrographic, geochemical and geochronological data. These results are expected to contribute to the improvement of knowledge about paleogeography of the central Brasilia Belt portion and to propose a new genetic interpretation and tectonic context for these rocks.

2 Geological Setting

The diachronic evolution of the Brasília Belt indicates two contrasting segments, the Northern and Southern with SW-NE and SE-NW regional trends, respectively (Araújo-Filho 2000). The Northern Brasilia Belt is formed by metasedimentary rocks, crystalline basement and the Neoproterozoic Goiás Magmatic Arc. The Southern Belt is formed predominantly of metasedimentary rocks of the Canastra, Araxá, Ibiá, Vazante and Bambuí groups, and also by part of the Goiás Magmatic Arc (Dardenne 2000; Valeriano et al. 2004).

The basement of the Southern Brasilia Belt is represented by three distinct areas, (1) the Campinorte Sequence, (2) the upper portion of the Greenstone Belts terrains in the Goiás Massif, and (3) the Silvânia Sequence. The Campinorte Sequence consists of metasedimentary rocks, interbedded with metachert, rhyolite and pyroclastic deposits, intruded by granite of the Pau de Mel Suite, dated (by U-Pb method in zircon crystals) between 2.16 and 2.18 Ga (Cordeiro 2014). The Goiás Massif consists of narrow greenstone belts and orthogneiss complexes of predominantly Archean age (Jost et al. 2005). The Artulândia Domain is represented by volcano-sedimentary sequence, including acidic volcanic rocks, which are intruded by 2.14 Ga tonalite by U-Pb method (Filgueiras 2015). The Silvânia Sequence is characterized by a narrow range of felsic metavolcanic rocks dated at 2.11 Ga, including amphibolites and metasediments, intruded by 2.0 Ga granites dated by Sm-Nd isotopic analyses (Piuzana 2002).

The basement of the northern Brasilia Belt consists of a sialic core consolidated in the Paleoproterozoic during the Rhyacian metamorphic event. Several authors have conducted studies on these terrains and different compartments have been proposed, such as Almas – Dianópolis (Cruz & Kuyumijian 1996; 1998), Almas – Conceição do Tocantins (Padilha 1984), Cavalcante – Teresina of Goiás (Botelho et al. 1993), among others. Fuck et al. (2014) proposed the Cavalcante – Natividade Crustal Block, which would include the entire sialic basement of the Northern Brasilia Belt, dividing it into two domains, Almas – Conceição and Cavalcante – Arraias.

More recently Cuadros (2017) and Cuadros et al. (2017) detailed the Aurumina Suite, which represents the main basement rocks in the basement of the North Brasilia Belt. This Suite is represented by heterogeneous rocks, commonly with peraluminous composition, including tonalite, granodiorite, granite and monzonite. All these intrusive bodies are straightly related to the schist of the Ticunzal Formation, at least in part considered the melting source of the granitoid liquids.

The study area is situated in the external central zone of the Brasília Belt (Figure 1A) northwestern of the Unaí/Minas Gerais. This orogenic belt is approximately 1,200 km long and 300 km wide with thrust and folding comprising nappes and structural basins and domes, with metamorphism and deformation increasing from east to west (Dardenne 2000). In the study area, outcrops the metasedimentary rocks of the Bambuí and Canastra groups (Figure 1B), and also the granitoids rocks (Figure 2). The Canastra Group includes Mesoproterozoic carbonate, quartzite, and phyllite in low-grade greenschist facies (Barbosa 1955; Barbosa et al. 1969), and the Bambuí Group is characterized by Neoproterozoic shale, siltstone, and carbonate (Dardenne 1978). Besides the Bambuí and Canastra groups, regionally, also occur rocks correlated to the upper Paranoá Group (Laranjeira & Dardenne 1990; Laranjeira 1992) and to the Quilombo Formation (Campos et al. 2021).

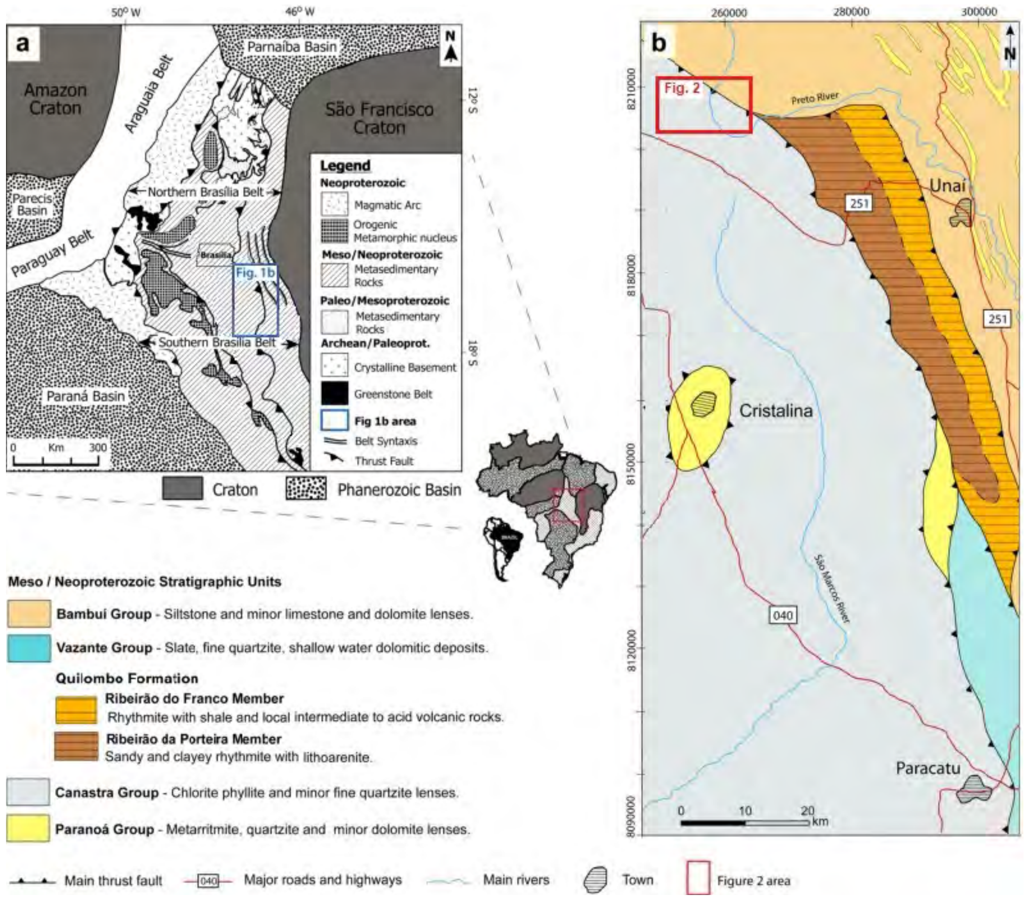

Figure 1 Schematic geologic maps showing: A. Location of the study area in South America, relative to the main cratons and in the Brasília Fold Belt, the blue polygon outlines the area of Figure 1B; B. Location study area in the southern Brasília Belt, the red polygon outlines the area of Figure 2 (modified from Dardenne 2000; Campos et al. 2021).

3 Analytical Procedures

The mineralogical identification and textural characterization of the rocks were performed using thin sections, previously prepared in the Lamination Laboratory of the University of Brasilia, under a petrographic transmitted light microscope.

Structural analyzes were carried out with the support of Open Stereo® and ArcMap® software. The data obtained in the field were treated in Stereogram and Rosette diagrams in order to show differences from granitic and supracrustal rocks deformational patterns.

In the ALS Laboratory, the total rock analyses consisted of spraying the samples in vibratory mill, using a special metallic pan, which were then heated to 1000 °C to determine mass loss on ignition. Major elements were determined by Inductively Coupled Plasma – Atomic Emission Spectrometry (ICP-AES) and trace elements by Inductively Coupled Plasma – Mass spectrometry (ICP-MS) and graph plotting using the Isoplot4 software.

U-Pb zircon analyses were carried out at the Geochronology Laboratory of the University of Brasília. The instruments used were a Thermo Finnigan Neptune multicollector inductively coupled plasma mass spectrometer coupled with a New Wave Instruments Nd:YAG solid-state laser with an output wavelength of 213 nm (LA-MC-ICP-MS). Zircon crystals collected from two outcrop areas, were previously prepared according the following steps: sample crushing, grinding, and sieving up to 30 Mesh fractions; density separation; magnetic separation (using a Frantz magnetic separator); hand-picking of zircon crystals using a magnifying glass; preparation of zircon mount for the Scanning Electron Microscope (SEM) analysis and LA-ICP-MS. Hand-picked zircon crystals were mounted in an epoxy disk, ground and polished, microphotographed in using a scanning electron microscope for cathode luminescence (CL). SEM imaging of zircon grains was obtained to analyzing textures, morphologies and to locate the spot for the analysis. The utilized ablation spots were 30 or 40 μm, and laser-induced elemental fractional and instrumental mass discrimination were corrected using the reference zircon (GJ-1) (Jackson et al. 2004), more details about the applied methods can be found in Bühn et al. (2009) and data interpreted using Chronus software.

4 Results

4.1 Geology of the Study Area and Petrography

The central Brasilia Belt, amidst the Bambuí group sedimentary rocks and next to the thrusts fronts, there are two outcrops of basement rocks. The first is located in most western part in the study area, and have approximately 400 x 300 m (named Area I; Figure 2) and the second, in the central region is about 200 x 250 m (named Area II; Figure 2).

These rocks that outcrop as rocky hills and blocks are light grey and silicified, medium-grained, displaying protomilonitic features. Petrographic studies indicated that the rock in Area I and Area II (Figure 3) are phaneritic tonalite and granodiorite, respectively. The Area I tonalite is holocrystalline, phaneritic, medium grained and porphyritic, with a modal mineralogical composition represented by highly saussuritized plagioclase (52%), quartz (20%), calcite (12%), chlorite (3%), microcline (5%), hornblende (3%), and epidote (2%). In addition, zircon crystals and iron oxide are observed as trace minerals representing about 3%.

The secondary minerals are represented by chlorite lamellae, as well as epidote and calcite, as anhedral crystals, measuring 0.5 mm on average. Plagioclase appear as elongated twinning crystals measuring between 0.5 and 3.0 mm, whereas quartz and microcline crystals are also anhedral, but varying from 0.1 to 1.0 mm and smaller than 0.5 mm, respectively. Hornblende relict crystals are weathered as a chlorite mass, measuring 1 mm on average.

The rocks collected in Area II are classified as granodiorite, and described as holocrystalline, phaneritic, medium grained and porphyritic inequigranular, but with slightly distinct mineralogical composition: quartz (35%), plagioclase (40%), and potassium feldspar (15%) as major minerals, in addition to calcite grains (5%) from modified plagioclase, zircon, and iron oxide grains (2%) as accessory minerals, as well as chlorite as a secondary mineral (derived from the alteration of biotite).

All the rocks observed in Areas I e II show protomilonitic features, including comminuting of primary crystals and quartz stretching and recrystallization.

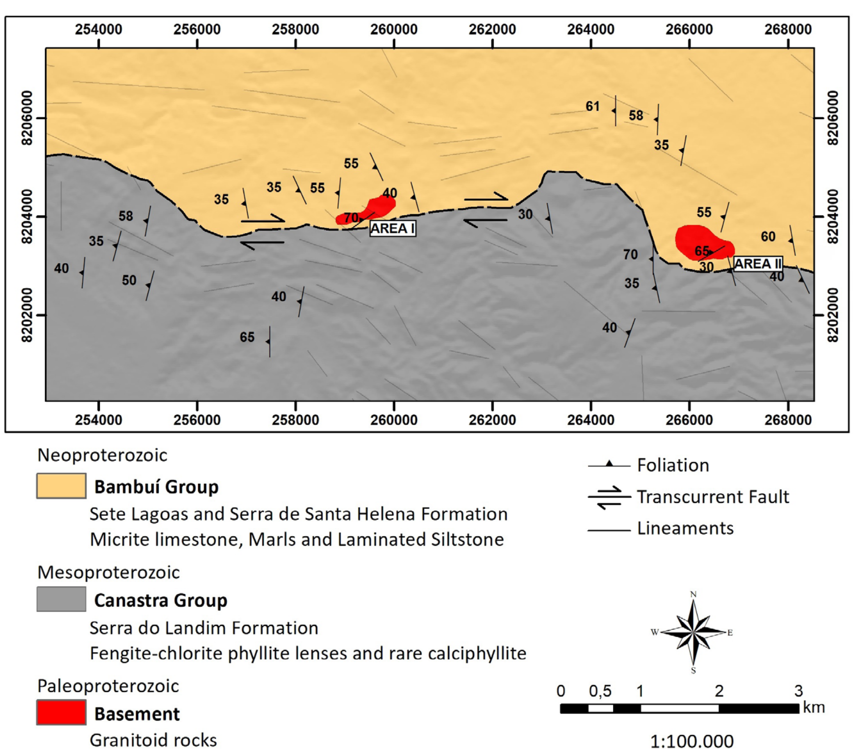

Figure 2 Simplified geological map of the study area.

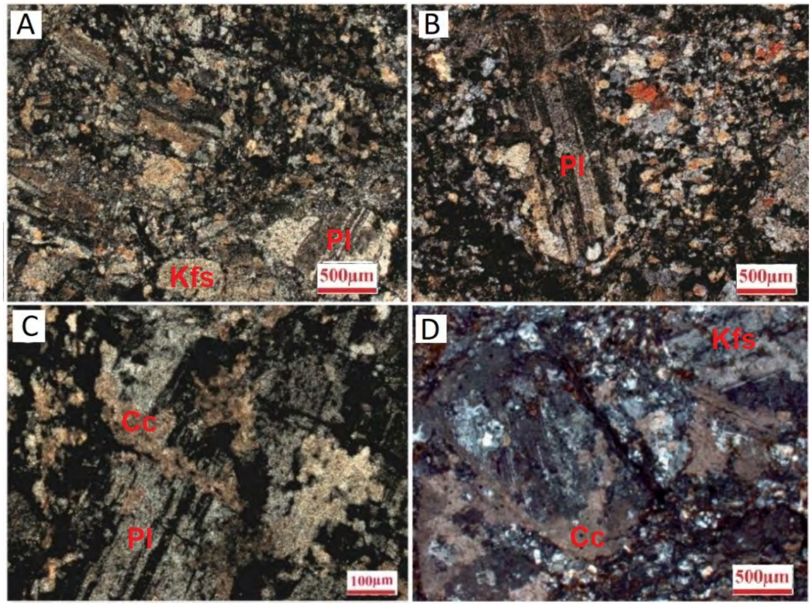

Figure 3 Representative petrographic features of tonalite and granodiorite from Area I and II: A. and B. General aspects showing inequigranular porphyritic texture, composed of plagioclase phenocrysts and matrix composed of quartz and K-feldspars; C. and D. Plagioclase crystals replaced by calcite.

4.2 Structural Analysis

The ductile-brittle and brittle deformation influence all units in the study area. The ductile-brittle tectonic is represented by thrusts, slaty cleavage, crenulation, and mineral stretch lineation, whereas the brittle tectonic is represented by spaced cleavage, kink bands and different families of faults and fractures resulting predominantly SE-NW structural lineaments.The Bambuí and Canastra groups are separated by regional thrusts, representing the convergent tectonic pattern prevalent in the external zone of the Brasilia Belt.

The foliations of the metasedimentary rocks have a similar pattern. When in the Bambuí Group is characterized by a mean strike of 270º dipping 56º (Figure 4D-E), in the Canastra Group is defined as a strike of 280º dipping 32º (Figure 4G-H). On the other hand, the granitoids show foliations planes with mean strike of 220º dipping 68º (Figure 4A-B), and these rocks exhibit mineral stretching lineation with preferential 130º/70º strike/dipping.

From the shaded relief images generated from the Shuttle Radar Topography Mission – SRTM satellite products (Figure 5), it is possible to observe two patterns of preferred lineaments direction (Figure 5 – Rose Diagram). There is the changing direction of the regional structural lineaments from N20-30W to N60-70W and again to N20-30W (next to the Unaí town). The inflection of the regional structures occurs exactly north of the basement exposition areas, what suggests the basement high controlling the deformation of the supracrustal successions.

4.3 Lithogeochemistry of the Basement Rocks

The data from Areas I and II (Table 1) were plotted together with samples from Aurumina Suite (Cuadros et al. 2017), to demonstrate the correlation between the studied area and the basement of the Northern Brasília Belt. In the TAS diagrams (Figure 6A), of alumina saturation (Figure 6B) and AFM (Figure 6C) there is a clear correlation in these two basement regions. Although there is a diversity of behavior in the REE of the Aurumina Suite, the rocks studied in this work show similar behavior when compared to some granitoids of the Northern Brasilia Belt (Figure 7A and 7B). In the Aurumina Suite there are granitoids classified as VAG and WPG, similar as in Areas I and II (Figure 8). In general, the oxides and alkalis of the granitoids in the study area exhibit a behavior similar to the granitoids in the Aurumina Suite as can be seen in Figure 9.

The six rock samples from the Areas I and II are classified as granite and monzonite according to the TAS diagram (SiO_2 x Na_2O+K_2O) (Figure 6A) and as metaluminous to peraluminous (Figure 6B). The samples collected in the Aurumina Suite, are chemically classified as granite, granodiorite, monzonite and diorite. The distribution of the samples related to the study areas in the AFM diagram (Kuno 1969; Irvine & Baragar 1971), characterizes the granitoids as a calc-alkaline series (Figure 6C), similar to the Aurumina Suite rocks (Cuadros et al. 2017).

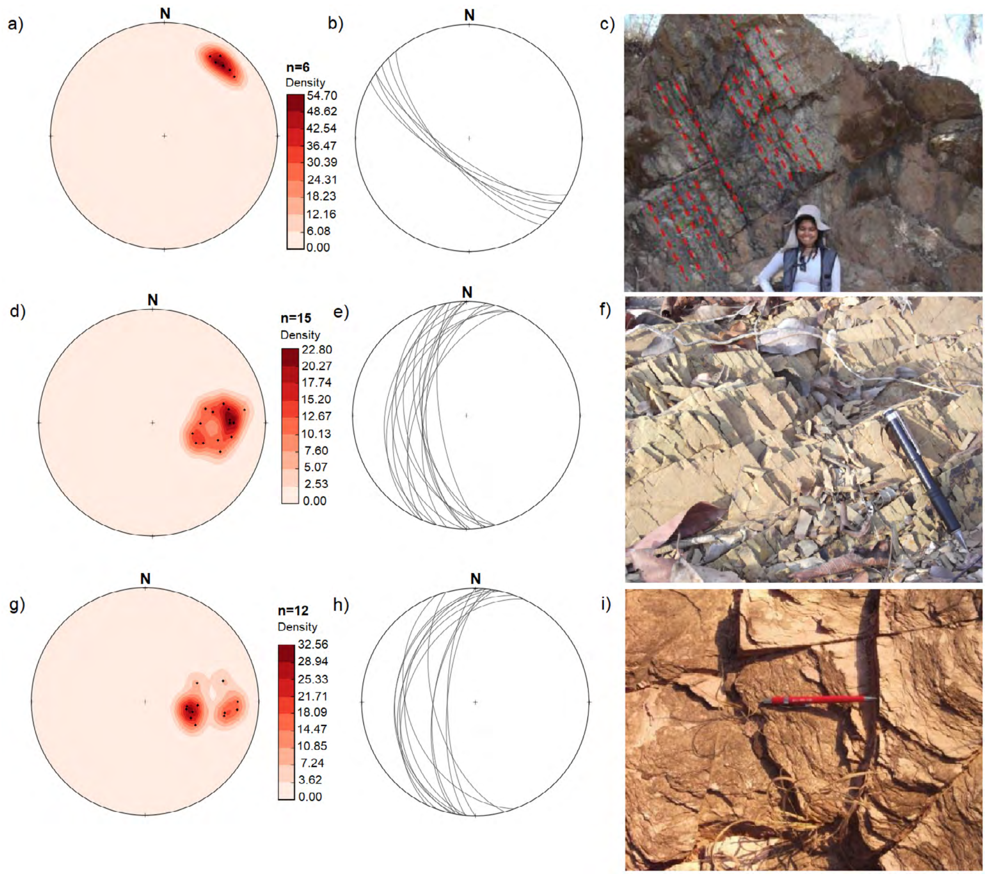

Figure 4 Poles of granitoid foliation plotted on Schmidt-Lambert stereogram, lower hemisphere: A. Points and isofrequency; B. Lines; C. Outcrop of basement rock in Area II. Poles of foliation of the Bambuí rocks plotted on Schmidt-Lambert stereogram, lower hemisphere; D. Points and isofrequency; E. Lines; F. Siltstone of the Bambuí Group, showing the pervasive spaced cleavages of the Poles of Canastra Group rocks foliation plotted on Schmidt-Lambert stereogram, lower hemisphere; G. Points and isofrequency; H. Points; I. Weathered chlorite phyllite from the Canastra Group.

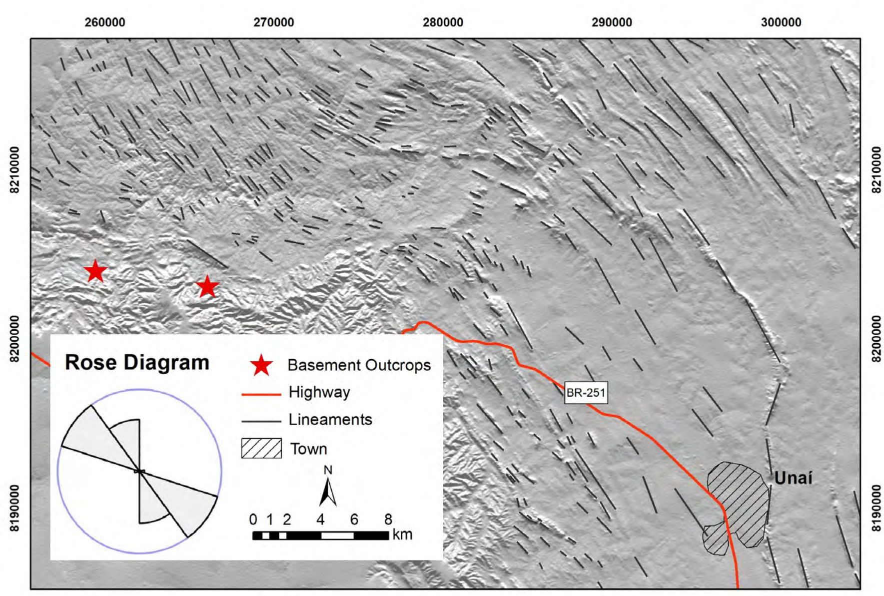

Figure 5 Regional structural map. The rose diagram indicates the preferential direction of the lineaments.

Table 1 Chemistry analysis results (major, trace and rare earth elements) from samples from the basement rocks (Areas I and II).

		SiO2	Al2O3	Fe2O3	CaO	MgO	Na2O	K2O	Cr2O3	TiO2
Area I	FM 02	59.8	15.4	5.73	3.05	3.25	6.11	1.47	0.02	0.84
	FM 20	55.1	15.45	6.12	4.1	3.66	6.1	0.86	0.022	0.83
	FM 21	75.6	13	2.19	0.41	0.49	4.51	2.97	0.002	0.19
	FM 22	75.6	12.55	1.33	0.49	0.36	4.57	3	<0.002	0.1
		MnO	**P2O5**	**SrO**	**BaO**	**LOI**	**Total**	**Ba**	**Ce**	**Cr**
	FM 02	0.11	0.25	0.03	0.13	4.18	100.37	1185	60.8	170
	FM 20	0.11	0.27	0.04	0.12	6.08	98.86	1095	52.4	170
	FM 21	0.03	0.04	0.01	0.12	1.53	101.09	1025	89.5	10
	FM 22	0.02	0.04	0.02	0.2	1.76	100.04	1830	53.9	10
		Cs	**Dy**	**Er**	**Eu**	**Ga**	**Gd**	**Hf**	**Ho**	**La**
	FM 02	2.12	2.27	1.42	1.58	19.5	3.62	3.9	0.45	26.4
	FM 20	1.98	2.78	1.32	1.59	18.8	3.62	3.7	0.45	24
	FM 21	0.47	11.85	7.49	1.27	21.3	9.76	6.8	2.32	43.8
	FM 22	0.75	3.45	1.93	0.79	16.8	4.16	3.9	0.69	30.8
		Lu	**Nb**	**Nd**	**Pr**	**Rb**	**Sm**	**Sn**	**Sr**	**Ta**
	FM 02	0.17	5.9	25.3	6.59	29.9	4.05	10	316	0.5
	FM 20	0.18	6.2	24.4	6.51	19.7	4.73	1	382	0.5
	FM 21	1.03	11.6	41.6	10.95	46.1	8.91	2	119	3.1
	FM 22	0.27	5.5	25.2	6.75	47.4	4.29	1	165.5	1.7
		Tb	**Th**	**Tm**	**U**	**V**	**W**	**Y**	**Yb**	**Zr**
	FM 02	0.42	5.04	0.19	1.49	116	70	13.5	1.21	155
	FM 20	0.52	3.86	0.22	1.31	115	154	14.6	1.19	144
	FM 21	1.74	10	1.04	2.29	14	1410	71.9	6.38	186
	FM 22	0.52	5.27	0.26	1.04	8	1270	33.1	1.79	104
Area II		**SiO2**	**Al2O3**	**Fe2O3**	**CaO**	**MgO**	**Na2O**	**K2O**	**Cr2O3**	**TiO2**
	FM 23	71.3	13.85	2.62	1.64	0.74	5.59	0.94	0.002	0.2
	FM 24	74	12.9	2.53	1.07	0.7	4.89	1.09	0.003	0.2
	FM 08	80.9	7.27	5.52	0.5	1.32	0.3	1.28	0.01	0.34
		MnO	**P2O5**	**SrO**	**BaO**	**LOI**	**Total**	**Ba**	**Ce**	**Cr**
	FM 23	0.03	0.06	0.01	0.02	2.89	99.89	198	93.9	20
	FM 24	0.02	0.05	0.01	0.02	3.02	100.5	210	74.1	10
	FM 08	0.18	0.09	<0.01	0.02	2.76	100.49	169	57.6	60
		Cs	**Dy**	**Er**	**Eu**	**Ga**	**Gd**	**Hf**	**Ho**	**La**
	FM 23	1.03	9.57	6.06	1.4	22	8.09	6.7	1.93	43.2
	FM 24	1.47	9.32	6.05	1.25	20.7	7.99	6.2	1.91	33.7
	FM 08	2.28	2.88	1.74	0.83	11.3	3.54	3.1	0.59	26.3
		Lu	**Nb**	**Nd**	**Pr**	**Rb**	**Sm**	**Sn**	**Sr**	**Ta**
	FM 23	0.88	11.6	43.5	11.2	41.3	9.34	3	125	2
	FM 24	0.9	10.7	34	8.86	45	7.22	2	110.5	1.7
	FM 08	0.22	16.2	23.3	5.95	60.9	4.48	3	33.9	0.9
		Tb	**Th**	**Tm**	**U**	**V**	**W**	**Y**	**Yb**	**Zr**
	FM 23	1.44	7.22	0.85	2.24	10	802	54.3	5.98	198
	FM 24	1.28	6.4	0.94	1.87	19	796	57.3	5.79	178
	FM 08	0.56	6.39	0.22	1.42	51	177	16.4	1.47	115

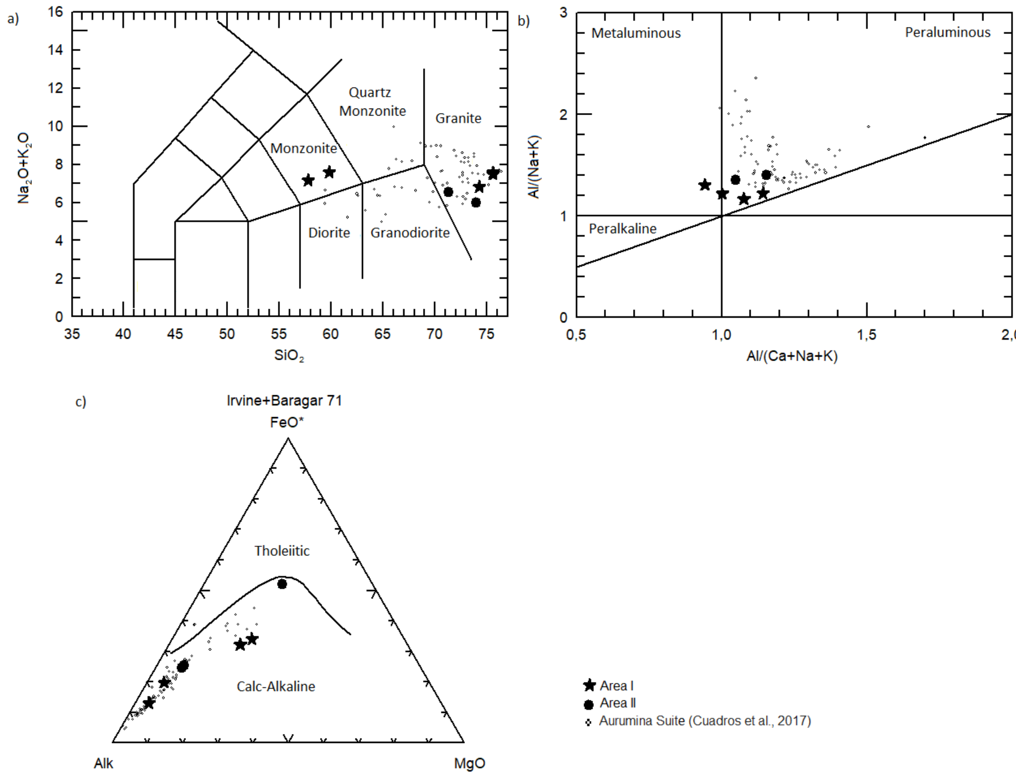

Figure 6 A. TAS diagram (Cox et al. 1979) showing the classification of the rock based on the percentage of silica versus total alkalis; B. Diagram for classification of rock in relation to saturation in alumina; C. AFM diagram (Irvine & Baragar 1971). * Area I, • Area II and · Aurumina Suite.

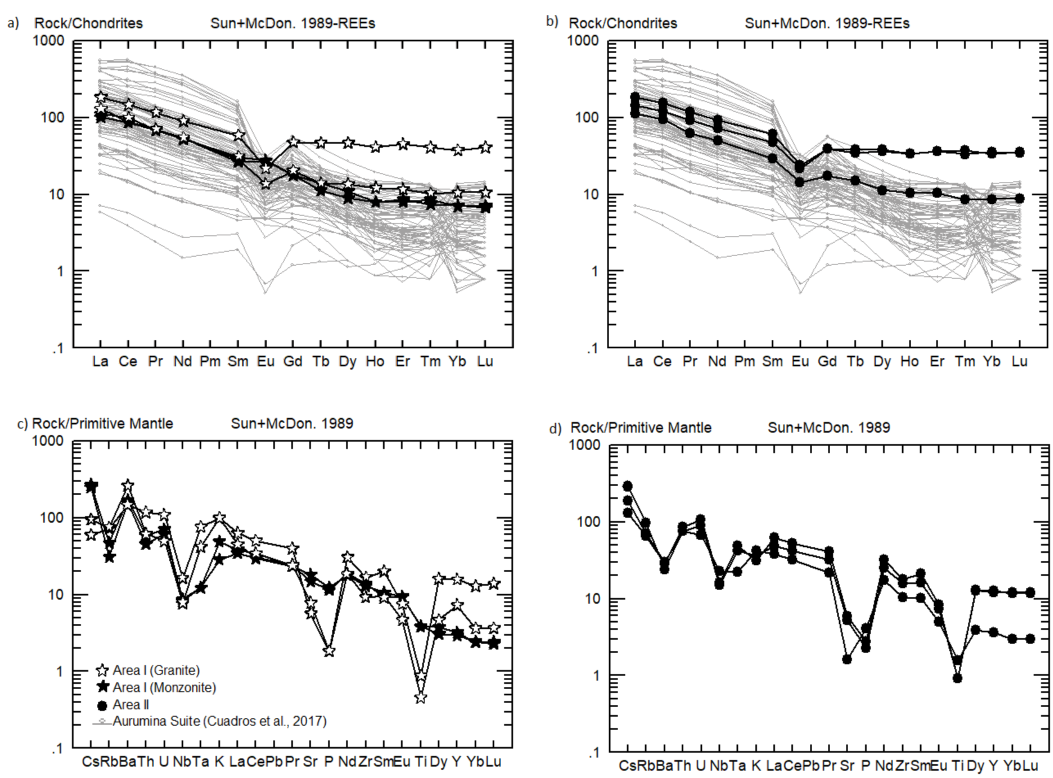

Figure 7 Distribution pattern of Rare Earth Elements normalized to chondrite: A. Area I and B. Area II. Multi-element diagram: C. Area I and D. Area II (Sun & McDonough 1989).

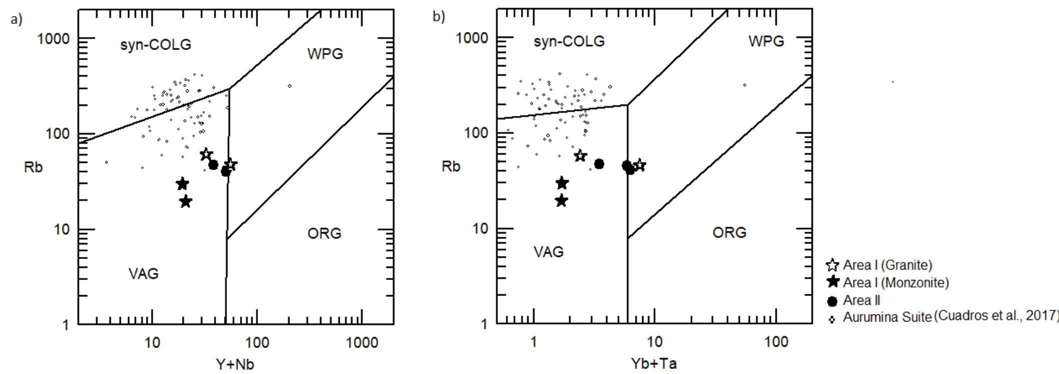

Figure 8 Geotectonic discrimination diagrams after Pearce et al. (1984): A. Y+Nb versus Rb; B. Yb/Ta versus Rb. Syn-Colg – Collision Granite; WPG – Within Plate Granite; ORG – Ocean Ridge Granite; VAG – Volcanic Arc Granite. * Area I, • Area II and · Aurumina Suite.

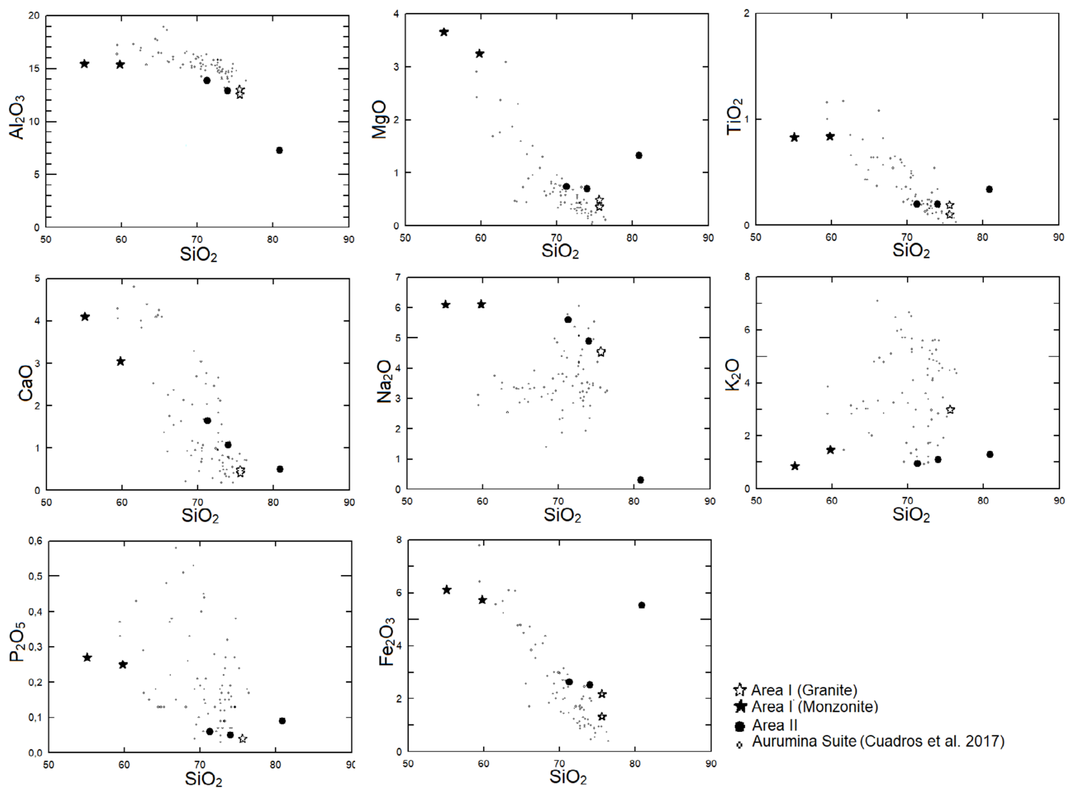

Figure 9 Geochemical features of the analyzed samples from Areas I and II and data from Cuadros et al. (2017). * Area I, • Area II and · Aurumina Suite.

According to the chondrite-normalized diagram (Sun & McDonough 1989), the Area I basement rocks show fractionation of heavy rare earth elements and enrichment in light rare earth elements with negative and positive Eu anomaly (Figure 7A). The multi-element diagram (Sun & McDonough 1989) shows that the large-ion lithophile elements (LILEs) are enriched in relation to the high field strength elements (HFS), with a slightly positive Ba anomaly and negative Rb, Nb, P and Ti anomaly (Figure 7C).

The rocks from Area II show similar behavior to the area I, with fractionation of rare earth elements and relative enrichment of light rare earth elements at the expense of the heavy ones, with negative Eu anomaly (Figure 7B). In the multi-element diagrams, a negative Sr and Ti anomaly was identified (Figure 7D).

Based on the diagrams proposed by Pearce et al. (1984) the rocks were classified in relation to its geotectonic formation environment (Figure 8). In the diagram Rb versus Y + Nb and Rb versus Yb + Ta most rocks plot in the field of volcanic arc granite (VAG) and two samples are characterized as within plate granite (WPG). These results contrast with the data from Cuadros (2017) in with the geochemical results plot mostly in the syn-collisional and volcanic arc granite.

A wide-ranging linear to curvilinear trend can be observed in Harker diagrams for Al_2O_3, CaO Fe_2O_3, and Na_2O (Figure 9). However, for MgO, TiO_2, and K_2O, clear trends are absent, and samples are scattered.

4.4 Geochronology

The images of scanning electron microscopy – SEM (Figure 10) show that the zircon crystals are bipyramidal prisms, colorless to translucent, euhedral and 100 µm long. After processing, the upper intercept ages determined from the discordant curve were 2,147.3 ± 4.5 [± 8.0] Ma for Area I and 2,140.3 ± 4.4 [± 8.2] Ma for Area II samples (Figure 11). The analyzed samples correspond to a monzonite and granite from Area I and Area II, respectively.

Table 2 presents analytical results of 30 and 28 grains from samples collected in the areas I and II, respectively. Due to the homogeneity of the zircon grains, a spot was made in each grain and all the analyzed spots were used to obtain the discordant curves. The ages of the lower intercept, respectively, 391 [± 110] Ma and 267 [± 49] Ma are interpreted as derived from loss of lead, with no geological significance whereas the upper intercept ages are interpreted as the zircon crystallization ages and, consequently, the age of the rocks.

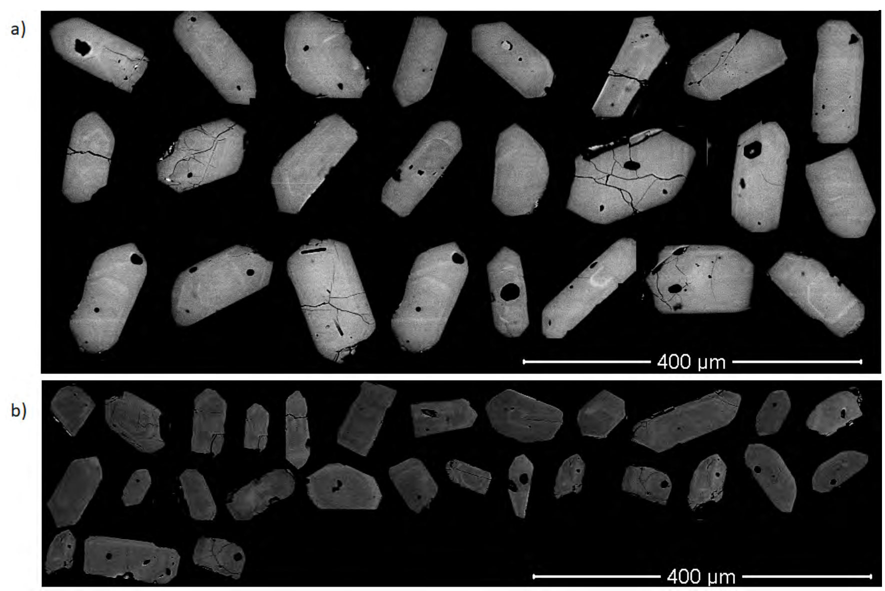

Figure 10 Images of scanning electron microscopy – SEM: A. Area I sample; and B. Sample from Area II. Spots made in the center of the zircon grains.

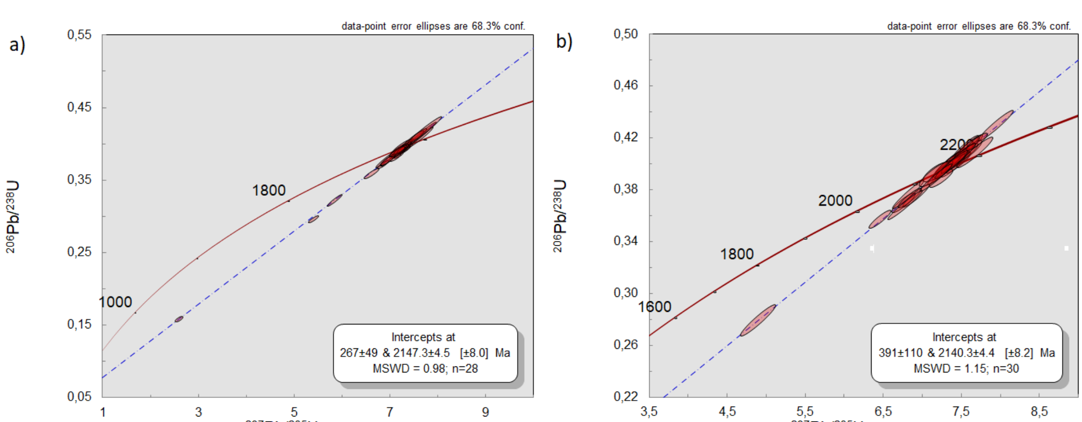

Figure 11 Ages of tonalite and granodiorite rocks of the Areas I and II obtained from the discordant curves: A. Area I sample; and B. Sample from Area II.

Table 2 Results of U-Pb dating (LA-ICP-MS) on zircons crystals of the basement rocks.

Sample Area I	f206 (%)	Th/U	$^{206}Pb/^{204}Pb$	1s% (%)	$^{207}Pb/^{206}Pb$	1s %	$^{207}Pb/^{235}U$	1s %	$^{206}Pb/^{238}U$	1s %	Error corr. (ρ)	$^{207}Pb/^{206}Pb$	2s abs	$^{206}Pb/^{238}U$	2s abs	$^{207}Pb/^{235}U$	2s abs	% U-Pb disc.
040-ZR30	0.002	0.229	98178	7.33	0.13284	0.52	7.377	1.76	0.4027	1.64	0.93	2136	18	2182	61	2158	31	-2.14
039-ZR29	0.003	0.265	126086	10.89	0.13342	0.44	6.918	1.65	0.3760	1.55	0.94	2144	15	2058	54	2101	29	4.01
038-ZR28	0.002	0.217	116835	9.83	0.13473	0.50	7.458	1.49	0.4015	1.36	0.91	2161	17	2176	50	2168	27	-0.70
037-ZR27	0.002	0.236	101096	5.67	0.13247	0.41	7.558	1.48	0.4138	1.37	0.93	2131	14	2232	52	2180	26	-4.75
036-ZR26	0.002	0.221	88579	11.62	0.13438	0.47	7.420	1.73	0.4005	1.62	0.94	2156	16	2171	60	2163	31	-0.70
035-ZR25	0.002	0.323	129309	5.25	0.13310	0.38	7.605	1.48	0.4144	1.39	0.93	2139	13	2235	52	2185	26	-4.47
034-ZR24	0.004	0.237	185133	9.03	0.13232	0.55	6.761	1.48	0.3705	1.32	0.89	2129	19	2032	46	2081	26	4.56
033-ZR23	0.001	0.221	76911	7.45	0.13480	0.55	7.240	1.36	0.3895	1.18	0.87	2161	19	2120	43	2141	24	1.89
030-ZR22	0.002	0.207	105140	6.70	0.13400	0.64	7.578	1.58	0.4101	1.40	0.88	2151	22	2216	52	2182	28	-3.00
029-ZR21	0.002	0.250	126389	4.21	0.13399	0.56	7.557	1.37	0.4090	1.19	0.87	2151	20	2210	45	2180	24	-2.77
028-ZR20	0.002	0.233	92009	8.52	0.13341	0.54	7.427	1.53	0.4037	1.38	0.90	2143	19	2186	51	2164	27	-1.99
027-ZR19	0.002	0.238	119273	7.16	0.13274	0.43	7.342	1.60	0.4011	1.50	0.93	2135	15	2174	55	2154	28	-1.86
026-ZR18	0.003	0.276	151825	10.33	0.13336	0.50	7.312	1.63	0.3976	1.51	0.92	2143	17	2158	55	2150	29	-0.71
025-ZR17	0.002	0.232	99668	10.35	0.13336	0.45	7.279	1.88	0.3958	1.79	0.95	2143	16	2150	65	2146	33	-0.33
024-ZR16	0.004	0.204	186110	8.90	0.13123	0.35	6.817	1.98	0.3767	1.91	0.97	2114	12	2061	67	2088	35	2.53
020-ZR15	0.003	0.297	134588	12.08	0.12678	0.86	4.894	3.02	0.2800	2.87	0.95	2054	30	1591	81	1801	50	22.52
019-ZR14	0.002	0.271	104876	21.83	0.13597	0.54	7.674	2.02	0.4093	1.91	0.95	2176	19	2212	71	2194	36	-1.62
018-ZR13	0.002	0.293	91524	7.37	0.13300	0.51	7.345	1.80	0.4005	1.69	0.94	2138	18	2171	62	2154	32	-1.56
017-ZR12	0.004	0.224	211517	8.40	0.13389	0.37	7.942	1.90	0.4302	1.82	0.96	2150	13	2307	71	2224	34	-7.30
016-ZR11	0.003	0.225	149250	7.60	0.13299	0.38	7.573	1.42	0.4130	1.31	0.93	2138	13	2229	49	2182	25	-4.25
015-ZR10	0.004	0.224	306881	29.96	0.13085	0.44	6.458	1.41	0.3579	1.29	0.91	2109	15	1972	44	2040	25	6.50
014-ZR9	0.003	0.192	189156	8.93	0.13360	0.42	7.694	1.17	0.4177	1.03	0.88	2146	14	2250	39	2196	21	-4.85
013-ZR8	0.002	0.292	102648	6.47	0.13406	0.46	7.426	1.15	0.4017	0.98	0.86	2152	16	2177	36	2164	20	-1.17
010-ZR7	0.002	0.229	69663	12.08	0.13196	0.89	7.175	1.57	0.3943	1.24	0.79	2124	31	2143	45	2133	28	-0.87
009-ZR6	0.001	0.243	80766	9.39	0.13243	0.91	7.178	1.98	0.3931	1.72	0.87	2130	32	2137	62	2134	35	-0.31
008-ZR5	0.002	0.306	224483	45.57	0.13252	0.47	6.838	1.48	0.3742	1.36	0.92	2132	16	2049	48	2091	26	3.86
007-ZR4	0.002	0.256	112680	7.11	0.13361	0.42	7.462	1.94	0.4050	1.86	0.96	2146	14	2192	69	2168	34	-2.16
006-ZR3	0.003	0.218	146186	10.29	0.13358	0.36	7.372	1.87	0.4003	1.80	0.96	2146	13	2170	66	2158	33	-1.15
005-ZR2	0.003	0.312	204076	8.20	0.13349	0.34	7.179	1.90	0.3900	1.83	0.96	2144	12	2123	66	2134	34	1.01
004-ZR1	0.006	0.235	320531	11.42	0.13328	0.33	6.777	2.12	0.3688	2.06	0.97	2142	11	2024	71	2083	37	5.51

Table 2 Results of U-Pb dating (LA-ICP-MS) on zircons crystals of the basement rocks.

Sample Area II	f206(%)	Th/U	$^{206}Pb/^{204}Pb$	1s% (%)	$^{207}Pb/^{206}Pb$	1s %	$^{207}Pb/^{235}U$	1s %	$^{206}Pb/^{238}U$	1s %	Error corr. (ρ)	$^{207}Pb/^{206}Pb$	2s abs	$^{206}Pb/^{238}U$	2s abs	$^{207}Pb/^{235}U$	2s abs	% U-Pb disc.
050-ZR30	0.0033	0.334	139842	11.02	0.13477	0.56	7.164	1.05	0.3855	0.80	0.77	2161	19	2102	29	2132	19	2.74
049-ZR29	0.0016	0.219	80069	9.19	0.13471	0.50	7.102	1.11	0.3823	0.92	0.83	2160	17	2087	33	2124	20	3.39
048-ZR28	0.0018	0.258	100992	6.38	0.13483	0.40	7.303	1.04	0.3928	0.89	0.85	2162	14	2136	32	2149	19	1.21
047-ZR27	0.0034	0.244	230104	13.45	0.13326	0.51	6.613	1.51	0.3599	1.37	0.91	2141	18	1982	47	2061	26	7.45
044-ZR26	0.0018	0.266	105850	6.79	0.13446	0.55	7.318	1.37	0.3947	1.20	0.87	2157	19	2145	44	2151	24	0.58
043-ZR25	0.0020	0.221	102467	10.62	0.13382	0.64	7.223	1.71	0.3914	1.55	0.90	2149	22	2129	56	2139	30	0.90
042-ZR24	0.0017	0.216	97999	7.24	0.13484	0.54	7.621	2.45	0.4099	2.36	0.96	2162	19	2214	88	2187	44	-2.43
041-ZR23	0.0043	0.257	259087	6.60	0.13396	0.40	7.600	3.15	0.4114	3.10	0.98	2151	14	2222	116	2185	56	-3.30
037-ZR21	0.0034	0.263	190821	8.06	0.13298	0.34	7.291	1.78	0.3977	1.71	0.96	2138	12	2158	63	2148	32	-0.96
036-ZR20	0.0028	0.300	146784	7.60	0.13095	0.38	5.837	1.77	0.3233	1.69	0.95	2111	13	1806	53	1952	30	14.46
035-ZR19	0.0025	0.312	117024	10.73	0.13383	0.70	7.180	1.64	0.3891	1.44	0.88	2149	24	2119	52	2134	29	1.40
032-ZR18	0.0025	0.248	131540	8.08	0.13243	0.53	7.166	1.74	0.3924	1.61	0.93	2130	19	2134	58	2132	31	-0.17
031-ZR17	0.0022	0.257	89423	12.58	0.13180	0.40	5.399	1.24	0.2971	1.11	0.90	2122	14	1677	33	1885	21	20.98
030-ZR16	0.0032	0.213	177703	7.18	0.13302	0.39	7.559	1.20	0.4121	1.08	0.89	2138	14	2225	40	2180	21	-4.04
029-ZR15	0.0018	0.218	107982	4.71	0.13414	0.43	7.305	1.23	0.3949	1.09	0.89	2153	15	2146	40	2149	22	0.33
026-ZR14	0.0025	0.310	173325	45.46	0.13251	0.74	7.241	1.90	0.3963	1.71	0.90	2131	26	2152	63	2142	34	-0.96
025-ZR13	0.0016	0.265	91167	6.20	0.13314	0.64	7.488	2.50	0.4079	2.39	0.96	2140	22	2205	89	2172	44	-3.06
024-ZR12	0.0045	0.210	266056	6.69	0.13336	0.57	7.718	3.07	0.4197	3.00	0.98	2143	20	2259	114	2199	55	-5.43
018-ZR11	0.0042	0.316	245517	7.60	0.13232	0.40	6.947	2.27	0.3807	2.20	0.97	2129	14	2080	78	2105	40	2.31
017-ZR10	0.0024	0.313	134337	7.84	0.13355	0.35	7.311	1.20	0.3970	1.09	0.91	2145	12	2155	40	2150	21	-0.47
016-ZR9	0.0047	0.369	241105	8.57	0.13381	0.32	7.256	1.07	0.3933	0.95	0.89	2149	11	2138	35	2143	19	0.49
015-ZR8	0.0030	0.256	161537	7.55	0.13372	0.33	7.272	1.13	0.3944	1.01	0.90	2147	12	2143	37	2145	20	0.20
012-ZR7	0.0064	0.345	365353	6.98	0.13342	0.40	6.849	1.09	0.3723	0.94	0.86	2143	14	2040	33	2092	19	4.82
011-ZR6	0.0024	0.261	121166	9.25	0.13306	0.40	7.206	1.19	0.3927	1.05	0.89	2139	14	2136	38	2137	21	0.15
010-ZR5	0.0084	0.614	1355	3.22	0.11759	1.33	2.586	2.10	0.1595	1.58	0.75	1920	47	954	28	1297	31	50.32
009-ZR4	0.0047	0.329	251701	7.33	0.13341	0.49	6.958	1.51	0.3783	1.37	0.91	2143	17	2068	48	2106	27	3.51
006-ZR3	0.0031	0.226	172015	6.67	0.13337	0.54	6.961	1.46	0.3785	1.31	0.89	2143	19	2069	46	2106	26	3.43
004-ZR1	0.0024	0.235	120395	9.94	0.13304	0.76	7.158	1.45	0.3902	1.18	0.81	2139	26	2124	43	2131	26	0.70

5 Discussions

The igneous rocks characterized in this study (in the Area I), located in the central portion of the Brasília Fold Belt, were initially described as an igneous intrusion known as the “Arrependido Body”, with U-Pb crystallization age of 785 ± 10 Ma (lower intercept) determined by Rodrigues (2008), however the upper intercept has an age of 2138 ± 44 Ma. The same author interprets these rocks as crustal origin due to the 2.24 Ga T_{DM} and the εNd (T) of -14.86 result from the Sm-Nd isotopic analysis.

Fieldwork, petrographic, geochemical and geochronological data allowed new interpretations to these exposures of igneous rocks among the basal sedimentary rocks at the Bambuí Group. The Paleoproterozoic age permit to conclude that these rocks are occurrences of the sialic basement, interpreted as paleogeographic highs, which were preserved after several geological processes. Both occurrences are arranged close to the thrust fronts at the tectonic contact between the Canastra and Bambuí groups; however the basement rocks are foliated in Area II and isotropic to protomilonite in Area I.

The foliation strike and dipping indicates the preservation of a pre-Brasiliano tectonic record. This data associated to the paleoproterozoic age allows concluding, that these rocks were submitted to the effects of the Rhyacian Orogenesis with deformation and metamorphic peak at about 2.0 Ga.

The geological evolution of the study region can be summarily described as follows:

– *Paleoproterozoic stage*: sialic basement consolidation in a collisional environment, about 2.14 Ga. This stage is compatible with the Aurumina Suite widespread in the north Brasília Fold Belt;

– *Statherian rifting stage*: crustal stretching and faulting responsible to keep low and high regional blocks, previous to the Brasiliano Belt development (Dardenne et al. 1999; Martins-Ferreira et al. 2018);

– *Consolidated sialic crust stage*: uplift, erosion and relief adjustment after exposure between the end of the Paleoproterozoic and early Neoproterozoic. At this stage high basement blocks are inheritance of the post rift relief;

– *Deposition of Neoproterozoic sediments stage*: first cycle of the Bambuí Group sedimentation over the crystalline basement;

– *Brasiliano Orogeny deformation stage*: tectonic transport of the Canastra Group (Mesoproterozoic age) over the Bambuí Group (Neoproterozoic) sedimentary rocks. At this stage the basement high acted as a rigid bulkhead controlling the regional deformation causing the inflection of the structure from NNW to N60-70E;

– *Recent stage*: after exposure, denudation, erosion and conformation of the current relief, where small areas of granitic rocks are exposed as little basement windows.

The basement of the Brasilia Fold Belt, consolidated during the Rhyacian event, is represented by three blocks: I) the volcanic arc environment related to the Campinorte Sequence dated at 2.2 Ga (Della Giustina et al. 2009); II) the active continental margin environment characterized by calc-alkaline granites dated as 2.2 Ga, and classified in Suites 1 and 2 (Cruz, Kuyumjian & Boaventura 2003); and, iii) the continental collision environment that generated the Aurumina Suite dated at 2.17 Ga (Botelho et al. 2006). Therefore, from the point of view of regional correlation, the basement rocks of the studied area present ages close to the Aurumina Suite, which constitutes much of the basement of the Northern Brasilia Fold Belt (Botelho et al. 1999; Cuadros et al. 2017).

All the geochemical results obtained from the samples of Areas I and II are quite similar to those data published by Cuadros et al. (2017). And the tectonic contact between the sedimentary rocks of the stratigraphic units cropping out in the area indicate that amalgamation of tectonic blocks caused the thrusting of the Bambuí Group over the phyllite rocks of the Canastra Group. The changing direction of the regional structural lineaments from N20-30W to N60-70W and again to N20-30W is attributed to the paleogeographic high of the Paleoproterozoic bedrock in the study region. This high block caused the development of a transpressive corridor that placed the low-grade metasediments of the Canastra Group over the Bambuí Group sediments. Because it is located in the external zone of the Brasilia Belt, the deformation is considered as thin-skinned type, that is, without involvement of the basement and thus, the foliation observed in the granitic rocks is attributed to a previous tectonic event. This assertion is corroborated by the foliation attitude of 220/68^o observed in the granitic rocks while the average foliation of the main supra crustal rocks next to the contact is 270/50^o.

These occurrences can also be interpreted as a source area to part of the supracrustal rocks in the region. According to Rodrigues (2008), the data of sedimentary rock provenance obtained from detrital zircon analysis show that the sources of the supracrustal rocks (metarhythmite with lithic greywacke, litharenite, and pelite) distributed in the region are dated between 1.7 and 2.2 Ga, with a very well defined peak at 2080 Ma. This age is very close to that regarded as the basement crystallization age (2147.3±4.5 [±8.0] and 2140.3±4.4 [±8.2] Ma) obtained in this work.

Despite the few numbers of measurements (due to the small outcrop areas), the Neoproterozoic deformation is compatible with a general mass transport from west to east and the tectonic movement related to the basement rocks is clearly from southeast to northwest. These deformation outlines are well-fitted to the Brasiliano and Ryacian collage, which took place, respectively in the Neoproteozoic (ca 600 Ma) and Paleoproterozoic (ca 2.0 Ga) (Cuadros et al. 2017; Martins-Ferreira et al. 2018).

Therefore, the fieldwork showing the absence of contact metamorphism in the adjacent supracrustal rocks, and the stratigraphic relationship with the pelitic rocks of the Bambuí Group, besides the zircon U-Pb ages, indicates that the observed granitic rocks cannot be related to an intrusive body, but must be interpreted as basement paleogeographic highs exposed as erosional windows in the region.

6 Conclusions

The granitoids occurring in northwestern of the Unaí town, in the State of Minas Gerais, are interpreted as outcrops of the basement of the Brasilia fold Belt. In the study area, the basement windows are arranged in two outcrops called Areas I and II that are observed flanked by the pelitic sedimentary rocks of the Bambuí Group, and next to the thrust controlling the contact between the Bambuí and Canastra groups.

The outcrops consist of igneous rocks of tonalitic, monzonitic, granitic and granodioritic compositions, with zircon U-Pb that yielded upper intercept ages at ca. 2.14 Ga. The association of field, petrographic, geochemical and geochronological data allows concluding that the occurrences of the igneous rocks directly in contact with sedimentary rocks are paleo highs of the basement.

Petrography, geochemical, geochronological data and structural pattern support the correlation of these rocks to the Aurumina Suite, which represents the basement prevalent in the north Brasilia Belt.

The ductile-brittle structures in the magmatic rocks are contrasting with relate to those observed in the sedimentary ones, what is interpreted as the register of the Rhyacian and Brasiliano orogenesis, respectively, preserved in the older and younger rocks.

These crystalline rocks acted as bulkhead, being responsible for the regional deformation inflection during the Brasiliano tectonic inversion. The paleo highs also acted as source areas to the younger sedimentary rocks deposited in the successive basins represented in the region.

7 References

Almeida F.F.M., Hasui Y., Brito Neves B.B., Fuck R.A. 1981. Brazilian structural provinces: an introduction. Earth-Science Reviews, 17(1/2):1-29.

Araújo-Filho, J.O. 2000, 'The Pireneus Syntaxis: an example of the intersection of two Brazilian fold-thrust belts in central Brazil and its implications for the tectonic evolution of western Gondwana', *Revista Brasileira de Geociências*, vol. 30, pp. 144-148.

Barbosa, O. 1955, 'Guia das Excursões', *IX Congresso Brasileiro de Geologia*, Araxá, pp. 3-5.

Barbosa, O., Batista, M.B., Dyer, R.L., Braun, O.P.G., Soriano, C.R., Arruda, M.E. & Corra, J.C. 1969, *Projeto Brasília – Goiás*, Relatório Final, Prospec/DNPM.

Botelho, N.F., Alvarenga, C.J.S., Meneses, P.R. & D'el-Rey Silva, L.J.H., 1999, 'Suite Aurumina: Uma suíte de granitos paleoproterozoicos, peraluminosos e sin-tectônicosna Faixa Brasília', in *Simpósio de Geologia do Centro Oeste*, SBG, Brasília, pp. 17.

Botelho, N.F., Bilial, E., Moutte, J., Fonteilles, M. 1993, 'Precambrian a-type tin-bearing granites in the Goiás tin province, central Brazil: a review', *Academia Brasileira de Ciências, Workshop sobre Magnetismo Granítico e Mineralizações Associadas, Rio de Janeiro*.

Botelho, N.F., Fuck, R.A., Dantas, E.L., Laux, J.H. & Junges, S.L. 2006, 'The Paleoproterozoic peraluminous Aurumina granite suite, Goiás and Tocantins, Brazil: geological, whole rock geochemistry and U-Pb and Sm-Nd isotopic constraints', in F.F. Alkmin & C.M. Noce, The *Paleoproterozoic record of the São Francisco Craton*, Field Guide and Abstracts, Ouro Preto, pp. 92.

Bühn, B., Pimentel, M.M., Matteini, M. & Dantas, E.L. 2009, 'High spatial resolution analysis of Pb and U isotopes for geochronology by laser ablation multi-collector inductively coupled plasma mass spectrometry (LA-MC-ICP-MS)', *Annals of the Brazilian Academy of Sciences*, vol. 81, no. 1, pp. 99-114, DOI:10.1590/S0001-37652009000100011.

Campos, J.E.G., Martins-Ferreira, M.A.C., Moura, F.G. & Chemale, F. 2021, 'Discovery of Precambrian deep-water turbidites and submarine volcanism in the Brasília Belt, Central Brazil: The Quilombo Formation', *Journal of South American Earth Sciences*, vol. 108, e103226, DOI:10.1016/j.jsames.2021.103226.

Cordeiro, P.F.O. 2014, 'Compartimentação geológica e geocronológica dos terrenos do embasamento norte da Faixa Brasília', Doctorate thesis, University of Brasília.

Cox, K.G., Bell, J.D. and Pankhurst, R.J., 1979. The Interpretation of Igneous Rocks. George Allen & Unwin Limited, London, 450 pp.

Cruz, E.L.C.C. & Kuyumjiam, R.M. 1998, 'The geology and tectonic evolution of the Tocantins granite-greenstone terrane: Almas-Dianópolis region, Tocantins State, Central Brasil', *Revista Brasileira de Geociencias*, vol. 28, no. 2, pp. 173-82.

Cruz, E.L.C.C. & Kuyumjian R.M. 1996, 'Chemical characterization of metabasalts and granitoids from the Almas-Dianópolis granite-greenstone terrane, central Brazil', *SBG Symposium Archaean Terranes South American Platform*, pp. 53-4.

Cruz, E.L.C.C., Kuyumjian R.M. & Boaventura, G.R. 2003, 'Low-K calc-alkaline granitic series of southeastern Tocantins State: Chemical evidence for two sources for the granite-gneissic complexes in the Paleoproterozoic Almas-Dianópolis Terrane', *Revista Brasileira de Geociencias,* vol. 33, no. 2, pp. 125-36, DOI:10.25249/0375-7536.2003332125136.

Cuadros, F.A. 2017, 'Relações petrogenéticas entre a Suíte granítica Aurumina e sua encaixante, a Formação Ticunzal, no setor setentrional da zona externa da Faixa Brasília', Doctorate Thesis, University of Brasília.

Cuadros, F.A., Botelho, N.F., Fuck, R.A. & Dantas, E.L. 2017, 'The peraluminous Aurumina Granite Suite in central Brazil: An example of mantle-continental crust interaction in a Paleoproterozoic cordilleran hinterland setting', *Precambrian Research*, vol. 299, pp. 75-100, DOI:10.1016/j.precamres.2017.07.029.

Dardenne, M.A. 1978, 'Síntese sobre a estratigrafia do Grupo Bambuí no Brasil Central', *Congresso Brasileiro de Geologia da SBG*, Recife, vol. 2, pp. 507-610.

Dardenne, M. A., Campos J.E.G., Alvarenga C.J.S., Martins F.A.L. & Botelho, N.F. 1999, 'A sequência sedimentar do Grupo Araí na região da Chapada dos Veadeiros, Goiás', *Simpósio de Geologia do Centro Oeste*, *Simpósio de Geologia de Minas Gerais*, Brasília, pp. 100.

Dardenne, M.A. 2000, 'The Brasília fold belt', in U.G. Cordani, E.J. Milani, A. Thomaz Filho & D.A. Campos (eds), *Tectonic Evolution of South America*, Rio de Janeiro, pp. 231-63.

Della Giustina, M.E.S., Oliveira, C.G., Pimentel M.M., Melo, L.V., Fuck, R.A., Dantas, E.L. & Buhn, B. 2009, 'U-Pb and Sm-Nd constraints on the nature of the Campinorte Sequence and related Paleoproterozoic juvenile orthogneisses, Tocantins Province, central Brazil', *Geological Society, London, Special Publications*, vol. 323, no. 1, pp. 255-69, DOI:10.1144/SP323.12.

Filgueiras, B.C. 2015, 'Depósito Vulcanogênico Polimetálico (Zn, Pb, Cu ± (Ag-Bi)) Artulândia, Arco Magmático Paleoproterozoico Campinorte, Brasil Central', Master Thesis, University of Brasília.

Fuck, R.A., Dantas, E.L., Pimentel, M.M., Botelho, N.F., Armstrong, R., Laux, J.H., Junges, S.L., Soares, J.E. & Praxedes, I.F. 2014, 'Paleoproterozoic crust-formation and reworking events in the Tocantins Province, Central Brazil: a contribution for Atlantica supercontinent reconstruction', *Precambrian Research*, vol. 244, pp. 53-74, DOI:10.1016/j.precamres.2013.12.003.

Irvine, T.N. & Baragar, W.R 1971. A guide to the chemical classification of the common volcanic rocks. Canadian Journal of Earth Sciences, 8:523-548.

Jackson S.E., Pearson N.J., Griffin W.L., Belousova E.A. 2004. The application of laser ablation-inductively coupled plasma-mass spectrometry to in situ U–Pb zircon geochronology. Chemical Geology, 211: 47–69.

Jost, H., Fuck, R.A., Dantas, E.L., Rancan, C.C., Rezende, D.B., Santos, E., Portela, J.F., Mattos, L., Chiarini, M.F.N., Oliveira, R.C. & Silva, S.E. 2005, 'Geologia e geocronologia do Complexo Uvá, bloco arqueano de Goiás', *Revista Brasileira de Geociências*, vol. 35, no. 4, p. 559-72, DOI:10.25249/0375-7536.200535559572.

Kuno,H., 1969. Pigeonite-bearing andesite and associated dacite from Asio, Japan. Amer. J. Sci., 267-A, 257-268.

Laranjeira, N.P.F. 1992, 'A Plataforma mista de siliciclásticos e carbonatos do Grupo Paranoá na região de Unaí – MG', Master Thesis, University of Brasília.

Laranjeira, N.P.F. & Dardenne, M.A. 1990, 'Relações estratigráficas e aspectos estruturais das sequências supracrustais aflorantes a NE de Unaí, MG', *Congresso Brasileiro de Geologia 1990*, Natal, pp. 23-33.

Martins-Ferreira, M.A.C., Chemale, F., Dias, A.N.C. & Campos, J.E.G. 2018, 'Proterozoic intracontinental basin succession in the western margin of the São Francisco Craton: constraints from detrital zircon geochronology', *Journal of South American Earth Sciences*, vol. 81, pp. 165–76, DOI:10.1016/j.jsames.2017.11.018.

Padilha, J.L. 1984, 'Prospecção de ouro na região nordeste de Goiás. Projeto Pindorama, DOCEGEO', *SBG, Encontro Regional do Ouro de Goiás*, Goiânia, pp. 78-95.

Pearce, J. A., Harris, N. W. & Tindle, A. G. 1984. Trace element discrimination diagrams for the tectonic interpretation of granitic rocks. Journal of Petrology 25, 956-983.

Piuzana, D. 2002, 'Contribuição à Evolução Crustal da Porção Central da Faixa Brasília: Estudos Isotópicos no Complexo Anápolis-Itauçu, Grupo Araxá, Sequência Vulcano Sedimentar de Silvânia e Granitoides Associados', Doctorate thesis, University of Brasília.

Rodrigues, J.B. 2008, 'Proveniência de sedimentos dos grupos Canastra, Ibiá, Vazante e Bambuí: um estudo de zircões detríticos e idades modelo Sm-Nd', Doctorate Thesis, University of Brasília.

Sun, S.S. & McDonough, W.F. 1989, 'Chemical and isotopic systematic of oceanic basalts: implications for mantle compositions and processes', in A.D. Saunders & M.J. Norry (eds), *Magmatism in Ocean Basins*, vol. 42, Geological Society of London, pp. 313-45.

Valeriano C.M., Dardenne M.A., Fonseca M.A., Simões L.S.A., Seer H.J. 2004. A evolução tectônica da Faixa Brasília. In: V. Mantesso-Neto, A. Bartorelli, C.D.R. Carneiro, B.B. Brito Neves (eds). Geologia do Continente Sul-Americano: evolução e obra de Fernando Flávio Marques de Almeida. Beca, São Paulo, p.575-593.

Author contributions

Florença das Graças Moura: formal analysis; methodology; validation; writing-original draft; visualization. **José Eloi Guimarães Campos:** conceptualization, supervision, review and editing.

Conflict of interest

The authors declare no potential conflict of interest.

Data availability statement

All data included in this study are publicly available in the literature.

Funding information

Not applicable.

Editor-in-chief

Dr. Claudine Dereczynski

Associate Editor

Dr. Gustavo Luiz Campos Pires

How to cite:

Moura, F.G. & Campos, J.E.G. 2023, 'Characterization and Geological Meaning of the Crystalline Basement Occurrence in the Unaí Region, Minas Gerais State (Central Brasilia Belt)', *Anuário do Instituto de Geociências,* 46:46563. https://doi.org/10.11137/1982-3908_2023_46_46563

Florença das Graças Moura, José Eloi Guimarães Campos

Characterization and Geological Meaning of the Crystalline Basement Occurrence in the Unaí Region, Minas Gerais State (Central Brasilia Belt)
Caracterização e Significado Geológico da Ocorrência do Embasamento Cristalino na Região de Unaí, Minas Gerais (Faixa Brasília Central)

Anuário do Instituto de Geociências
vol. 46, 46563, 2023
Universidade Federal do Rio de Janeiro,
ISSN: 0101-9759
ISSN-E: 1982-3908

DOI: https://doi.org/10.11137/1982-3908_2023_46_46563